Examination of an externally loaded leaking flange joint for leaking using finite element analysis

Sam Gilbert, Brian Hoover, Chidhambara Kalusulinga, Michael Regan, and **Bijoy J. Verghese**
Department of Mechanical Engineering, University of Illinois at Urbana Champaign

ABSTRACT

Bolted flange joints heavily utilize gaskets to create a seal in pipelines. Not only do gaskets experience high operating pressures and external loads, but also elemental exposure affects the integrity of the gasket seal. When seal performance fails, alternative flange joints must be examined. This investigation explores the feasibility of replacing an existing spiral wound gasket on a flange joint with a ring type joint for high pressure pipelines evaluated with Abaqus software and with an author-created MATLAB finite element method solver.

Keywords: flange joint, finite element analysis, bolted joint leak analysis, spiral wound gasket, ring type joint (RTJ)

1.0 Introduction

A leak in the first joint, a 12" 900# RF flange joint, was discovered in an offshore high-pressure gas pipeline feeding an onshore facility. Investigation of the joint identified minor gas leakages in the joint's spiral wound gasket (Figure 1.1). A spiral wound gasket is not recommended to be utilized under high pressures and high external loads by the American Petroleum Institute (API) [13]. An additional root cause of the gas leakage was identified as soil settlement across the pipeline, resulting in a high differential external load on the flange joint. Although leakage risks were mitigated via reduction in gas operating pressure and the installation of a temporary clamp on the joint, a long-term, permanent solution was needed.

The pipeline runs over a hundred kilometers in length and is 12" in diameter. The minor gas leakage was observed at an operating pressure of 60 bar. Further reduction of the operating pressure to 40 bar initially indicated no further leakage, however during verification, gas leakage was still observed at 29.6 bar operating pressure. Presently, the plant operates at 30 bar with a clamp on the flange joint.

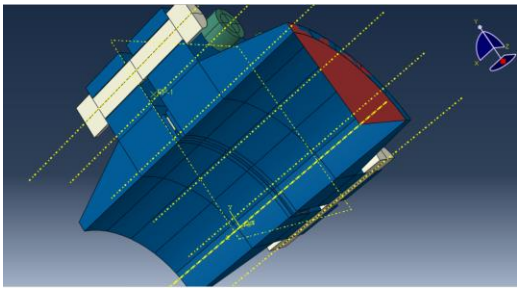

Figure 1.1: Model representation of existing joint and its spiral wound gasket

This investigation explores the feasibility of replacing the existing flange joint and its existing spiral wound gasket (Figure 1.2) with a ring type joint (Figure 1.3).

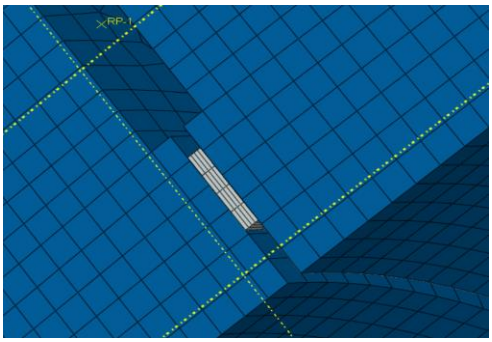

Figure 1.2: Close-up of model representation of existing spiral wound gasket

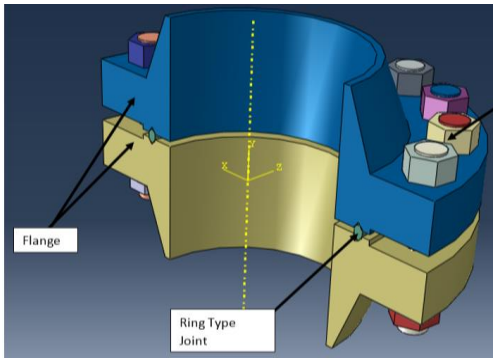

Figure 1.3: Proposed ring type flange joint

In addition, this study explores the API RP 14E [13] recommendation for the use of ring type joints in high pressure joints as a permanent solution for the onshore upstream facility. A comparison between the raised face and ring type joint (RTJ) was made under the same loading conditions simulating the actual load the joint is subjected to. This report will be used as a justification for the costly permanent modification proposed to the site team.

Additionally, a finite element solver was written in MATLAB to compare to a two-dimensional model of the flange under the bolt load. After exporting the sketch from Abaqus a mesh was generated with GMSH, and the displacements evaluated were comparable to the results of the similar problem in Abaqus.

2.0 Geometry

Two types of geometries were used for analysis, a raised face flange and a ring groove type flange. The geometry of the 12" 900# flange dimensions was extracted from MSS-SP-44: Pipe Flanges and Flanged Fittings [1]. CGI style spiral wounded gasket dimensions and oval type ring gasket R-57 dimensions were extracted from ASME B16.20: Metallic Gaskets for Pipe Flanges [2]. The basic minor diameter of the 1-3/8" bolt diameter was used for the analysis. Also, 1-3/8" nut minimum across flat dimension used to simplify the shape from hexagonal to circular. The component geometries shown in Figure 2.1 and 2.2 were simplified in Abaqus to help in the preparation of a well-structured mesh. This typically involved removal of cosmetic and non-structurally significant features such as small chamfers and fillet radii in noncritical regions. As this is axis symmetric model and to reduce the analysis complexity and computational time, 1/40th of geometry and loading was utilized. Commercial software Abaqus (teaching version) has been used as a finite element solver.

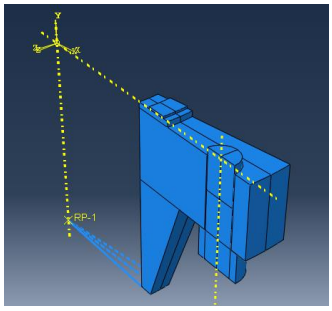

Figure 2.1: Raised face flange model

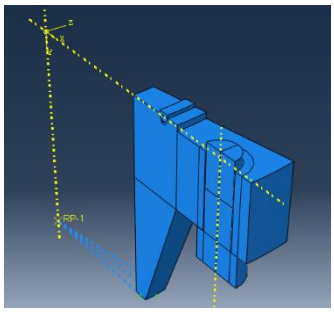

Figure 2.2: Ring type joint flange model

3.0 Material properties and data

Part	Material	Young's modulus	Poisson's ratio	Co-efficient of thermal expansion
Flange	ASTM A694 Gr.65	203395	0.3	1.265e-5
Ring gasket	Soft iron	200000	0.26	1.8e-5
Spiral gasket	Graphite filled SS 316	18000	0.3	1.8e-5
Fastener	ASTM A320 Gr.7	204000	0.3	1.265e-5

Gasket non-linear material properties

Pressure versus closure behavior could be directly applied to apply to characterize the gasket material in Abaqus. Mechanical characteristics of the gasket material were carried out by a load compressive mechanical test as presented in reference [3] for this analysis. Abaqus software had a provision to input the load compressive mechanical test data. Figure 3.1 and Figure 3.2 show the material properties for spiral wound gaskets and ring gaskets. The non-linear compression behavior with two different unloading curves was considered in the present analysis. If unloading occurred at an intermediate point, the unloading curve was interpolated from neighboring curves. Reloading was assumed to take the same path as the unloading curve for repeated load cycles.

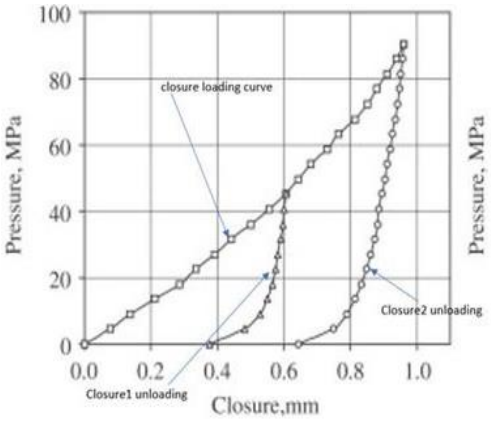

Figure 3.1: Spiral wound gasket closure data

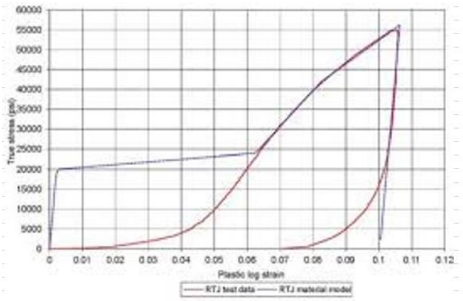
Figure 3.2: RTJ gasket closure data

4.0 Discretization and meshing

4.1 Meshing

The raised face flange was meshed with first order 4-noded tetrahedral elements (Type C3D4R). The fasteners and gaskets at the flange interface were modeled with 8-noded hexahedral elements (Type C3D8R), and the end cap was modeled as a rigid element to transfer the loads to the flanges.

For the RTJ flange model:

- The bolts were meshed with C3D8 an 8-node linear brick
- The RTJ gasket and the flange were modeled with C3D8R an 8-node linear brick, reduced integration, hourglass control
- The end cap was modeled as a rigid element

The model also would be more accurate if the end cap could be modeled to transfer the load properly simulating the conditions at the field.

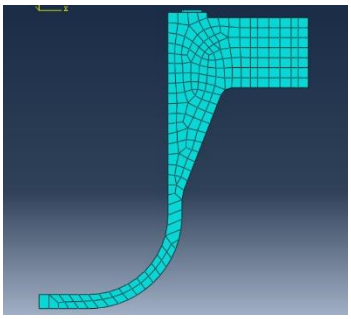

Although reduced integration was used for a quick computation and convergence, further study is recommended with the use of a denser mesh and C3D4 and C3D8 elements for more accurate results. Due to the limitation of the number of nodes, these could not be achieved in this study.

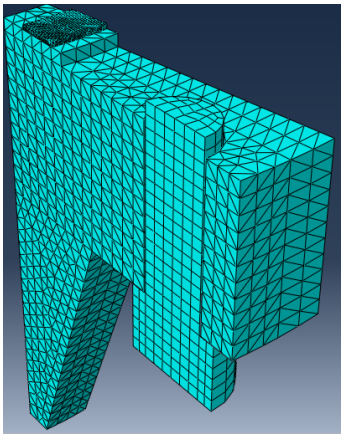
Figure 4.1.1: Mesh

4.2 Contact elements

The Abaqus software's default contact elements were modeled with the following properties:

- Tangential behavior: Rough
- Normal behavior: Hard contact

The contact elements were generated between the faces of the nuts mating with the flanges. Likewise, contact elements were generated between the gasket faces and the corresponding faces on the flanges. These were modeled with small sliding and surface-to-surface contact.

Further improvements were suggested for these due to the limitation of the number of the nodes to 20,000 nodes the teaching version of the Abaqus finite element analysis software used for this study. The software's default was used to get convergence in the model.

5.0 Boundary conditions

The symmetry sectional faces of the flange, bolt and gaskets were constrained in the U_z translation in the global and the skewed axis on the other end.

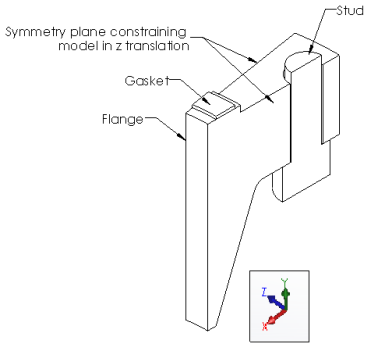

Figure 5.1: Symmetry constraint

The top face of the gasket and stud were constrained in the U_y translation.

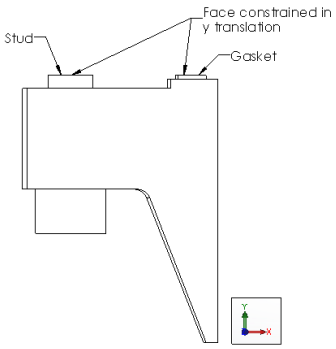

Figure 5.2: Y-axis constraint

6.0 Loading conditions

The model was subjected to six individual unit loads: bolt makeup load, internal bore pressure with the associated pressure end load, temperature, tension of axial pipe stress, and a bending moment that resulted in stress at the extreme fiber of the pipe.

6.1 Bolt load

The applied bolt load was 115,598 N x 2 halves. The data was obtained from the actual torque applied at site during construction to achieve the tension in the bolt (231,196 N).

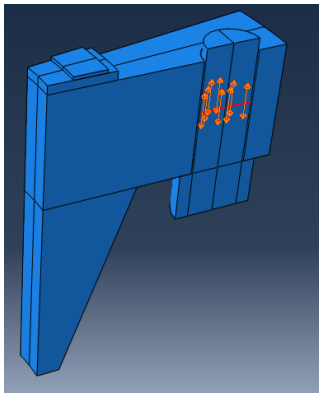

Figure 6.1.1: Bolt load

Table 6.1.1

Dimension of bolts and nut as per ASME B 18.2.2		
Description	**Bolt load**	**Units**
full bolt (Load)	231196	N
half bolt	115598	N
bolt hole d1	38.1	mm
bolt head d2	54.1	mm
area = pi()(d2^2-d1^2)/4	1158.62	mm2
bolt pressure on above area (Load /Area)	199.544	mpa

The flange bolt hole diameter was 38.1mm (refer to MSS SP 44), and the nut outside diameter was 53.8mm (refer to ASME B18.2.2) as shown in Figure 6.1.2.

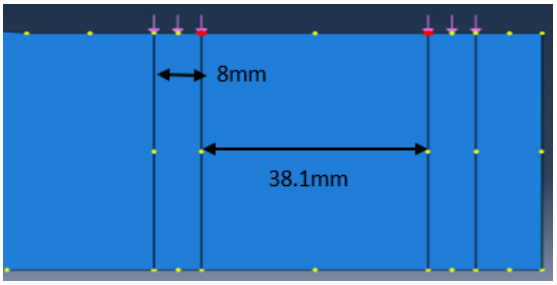

Figure 6.1.2: Modeled bolt dimensions

For the 2-D model, this tension in the bolt was converted to the pressure load transferred to the flange by the nut. This was calculated to be 199MPa for the 2-D model.

6.2 Pressure

The applied bore pressure was 10MPa. The pressure was applied along the bore and to the face of the flange up to the seal diameter.

The corresponding axial pressure end load of 199.619MPa was applied at the hub end of the flange.

Table 6.2.1: Axial pressure load calculation

Axial Pressure Load Calculation				
Pipe OD	12.74	=	323.596	mm
Pipe wall thk	15.9	mm		
Pipe ID	291.796	mm		
DESIGN PRESSURE	10	Mpa		
STRESS, P*D/(4*t), =	45.8799	Mpa		
Force, F=stress * area	3068109	N		
therefore, for one section	76702.7	N	76702.7	N
Uniformly distributed Axail Pressure Load	199.619	N/mm2	199.619	Mpa
Note: Negative load applied				

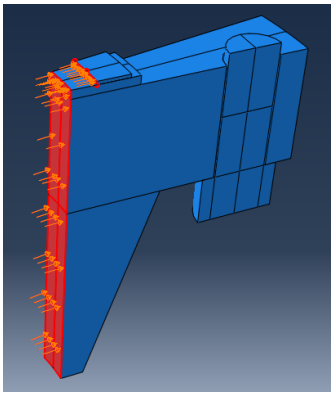

Figure 6.2.1: Internal Pressure

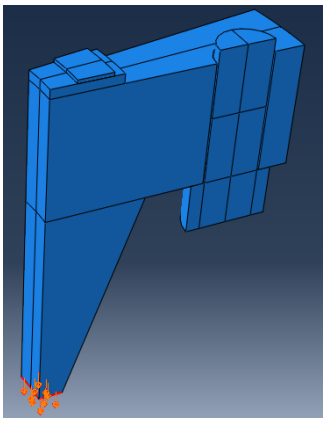

Figure 6.2.2: Pressure end load

6.3 External axial force due to soil settlement

The axial force, F_y was 12,560 N.

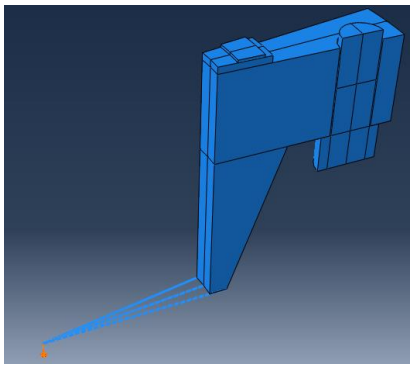

Figure 6.3.1: Axial force and Moment

6.4 Bending moment due to soil settlement

The moment applied, M_z was -7.548E+007Nmm.

6.5 Operating temperature

The maximum and minimum temperature was 60°C and 21°C, respectively.

7.0 Assumptions and limits

All materials were assumed to be isotropic. Also, the materials were assumed to be without defect, having not experienced any previous loading and unloading cycles.

The existing gasket had an SS316L inner and outer ring. This was however, not modeled as it was not a sealing element. The outer ring was only used to center the gasket, and the inner ring was used to protect the flange from overtightening.

8.0 Finite element analysis

This investigation performed the following analyses:

1. A hand calculation for raised face flange joint in accordance with ASME Section VIII division 1 rules with the Kellogg Pressure Equivalent Method to convert the external load to pressure equivalents.
2. 3-D Analysis on the existing spiral wound gasket joint using Abaqus software
3. 3-D Analysis for the proposed RTJ Gasket joint using Abaqus software
4. 2-D Analysis on spiral wound gasket joint using Abaqus Software
5. The team also coded their own solver using MATLAB

For both the 2-D solvers, the team modeled a two-dimensional slice of one side of the existing gasket of the raised face (RF) and modeled the bolt load case only to compare the results of the solvers. Contact modeling was not considered presently in the team's coded solver.

The hand calculation was done to check the raised face flange joint with the maximum allowable stress on the flange in accordance with MSS-SP-44 in the operating conditions and initial gasket seating conditions.

However, for the FEA analysis the actual yield stress of the materials was used to check the flanges and bolts. Closure pressure of spiral wound gaskets were extracted from previous research papers [7], and for RTJ, no research materials were found. Reputed vendor catalogues were used to check the allowable minimum/maximum gasket closure pressures required for sealing.

8.1 3-D Abaqus solver

A. Spiral wound gasket

For the three-dimensional (3-D) models, the stress and displacement states of the two models were considered three-fold: loading stress at bolt-up, relaxation at pressurization, and bending moment application with a temperature increase. Figures 8.1.1-8.1.6 show the initial stress and displacement analyses of the current, spiral wound gasket at these states in both an overhead and profile view. The maximum Von Mises stress on the gasket occurred after bolt-up and was located on the outside edge of the gasket with a calculated value of 385.7MPa. Also, the gasket was displaced by 0.059mm at this location. The maximum displacement of the gasket occurred on the inside edge, with a calculated value of 0.068mm. After relaxation due to pressure, the stress in this area remained as the local maximum, but the calculated value due to pressurization decreased to 173.3MPa while the displacement at this decreased to 0.041mm. The maximum displacement decreased to 0.064mm, again occurring along the inside edge. Finally, after applying the external bending moment and external force due to soil settlement, the stress in this area decreased further to 137.7MPa while the local displacement increased to 0.043mm. The maximum displacement also increased, to a value of 0.066mm along the inside edge.

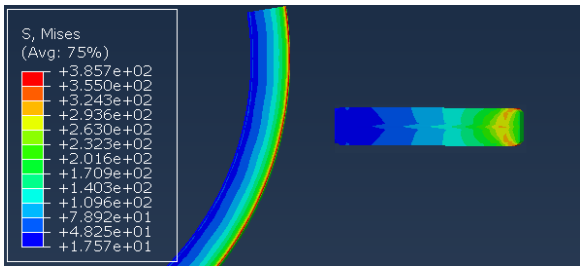

Figure 8.1.1: Spiral Wound Gasket Stress after Bolt-Up

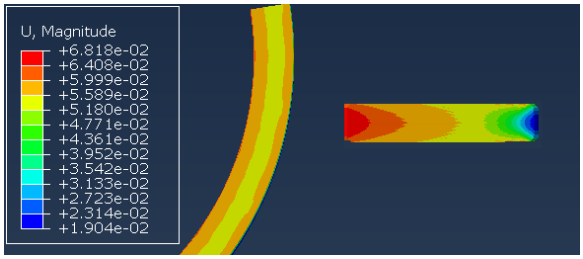

Figure 8.1.2: Spiral Wound Gasket Displacement after Bolt-Up

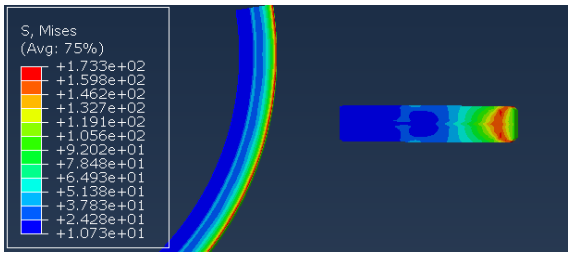

Figure. 8.1.3: Spiral Wound Gasket Stress with Pressure

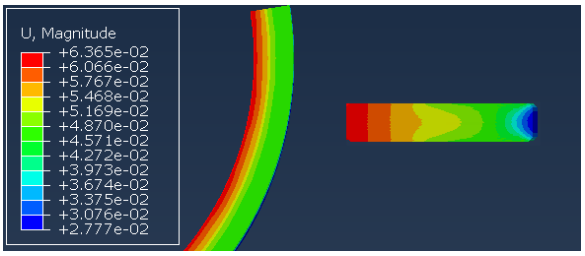

Figure 8.1.4: Spiral Wound Gasket Displacement with Pressure

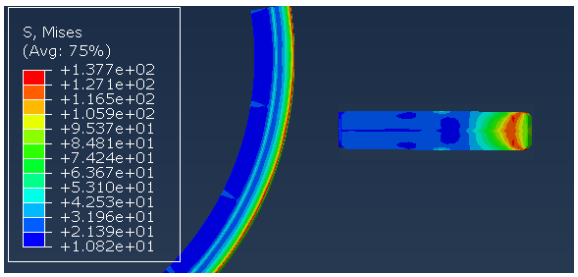

Figure 8.1.5: Spiral Wound Gasket Stress w/ Moment

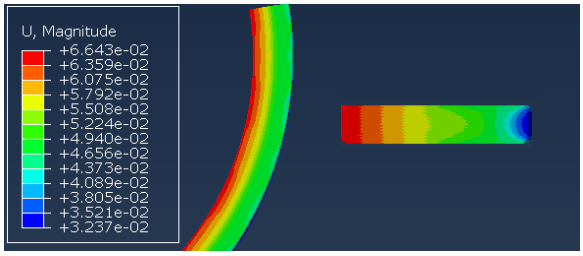

Figure 8.1.6: Spiral Wound Gasket Displacement with Moment

B. Ring type joint

A similar model was developed using a ring-type joint (RTJ) and the stress and displacement analyses at the three states are shown in Figures 8.1.7-8.1.12. For the RTJ, the maximum Von Mises stress occurred on the inside of the gasket where it contacts the flange with a calculated value of 480.0MPa. The gasket was displaced by 0.41mm at this location during this step in the process. The maximum displacement occurred on the outside of the gasket, where it contacts the flange, and was calculated at 0.45mm. Once pressurized, the maximum stress decreased to 331.8MPa while the displacement at this max stress decreased to 0.09mm and the maximum displacement remained unchanged. Finally, the applied moment and change in temperature increased the local stress to 322.3MPa as the local and max displacement did not significantly change.

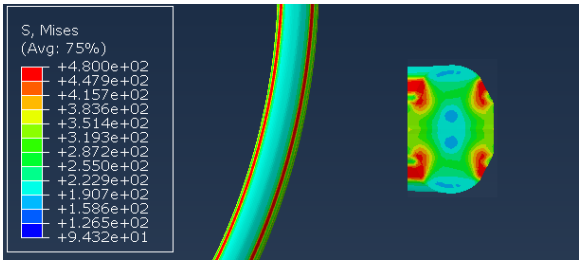

Figure 8.1.7: RTJ Gasket Stress after Bolt-Up

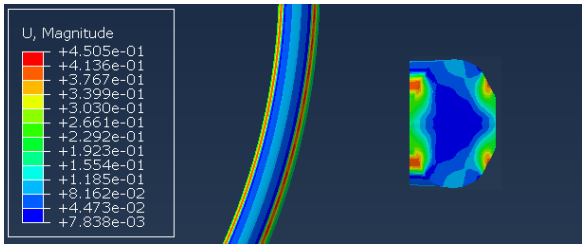

Figure 8.1.8: RTJ Gasket Displacement after Bolt-Up

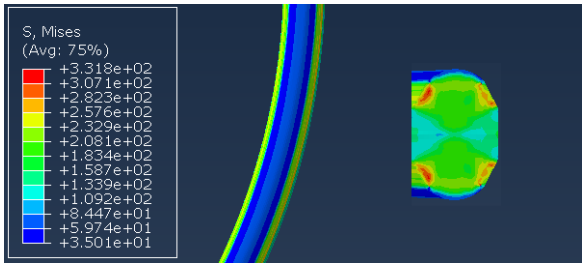

Figure 8.1.9: RTJ Gasket Stress with Pressure

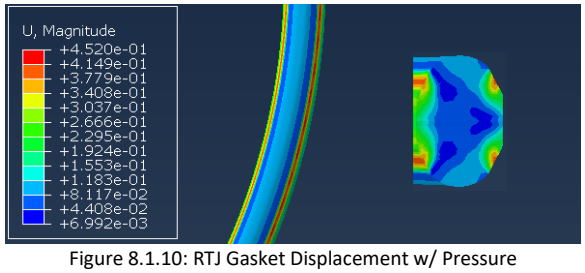

Figure 8.1.10: RTJ Gasket Displacement w/ Pressure

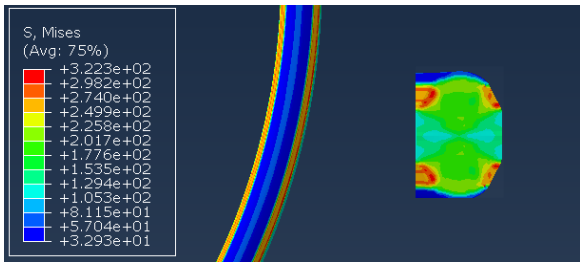

Figure 8.1.11: RTJ Gasket Stress with Moment

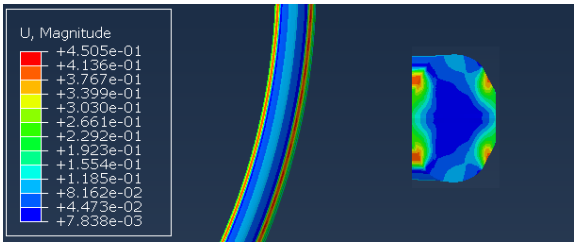

Figure 8.1.12: RTJ Gasket Displacement with Moment

8.2 2-D Abaqus solver

A two-dimensional (2-D) model was created of the spiral wound gasket flange joint using Abaqus finite element analysis software. The flange was considered as symmetric to create a 2-D slice of the cross section of the flange joint and designed with 4-node bilinear plane stress quadrilateral elements (CPS4) as shown in Figure 8.2.1.

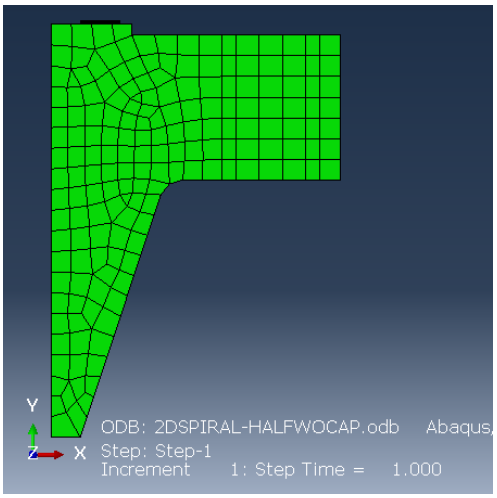

Figure 8.2.1: 2-D Abaqus FEA model of spring wound gasket flange joint

A y-direction symmetric boundary condition was set for the top face of the gasket, which created a symmetry constraint about a plane of constant y-coordinate. A x-direction symmetric boundary condition was set for the inside of the flange, which created a symmetry constraint about a plane of constant x-coordinate.

Two loads from the bolts on the flange were modeled as mechanical forces, and the gas within the pipeline was modeled as a uniform pressure on the inside surface of the proposed flange joint as shown in Figure 8.2.2. The contact forces of the gasket were modeled as an equivalent pressure on the surface of the RTF. Under such loading conditions, the maximum displacement of the flange occurred at the piece's outer edges where the bolts were loaded as shown on the plotted contours in Figure 8.2.3 with a maximum displacement of 0.2327mm.

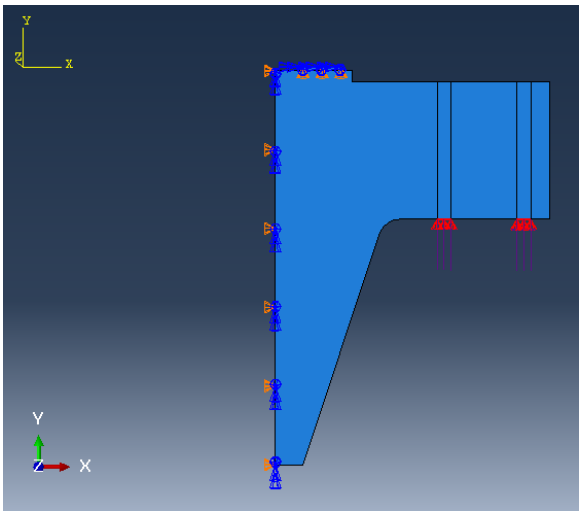

Figure 8.2.2: Loading conditions of 2-D Abaqus FEA model of proposed flange joint

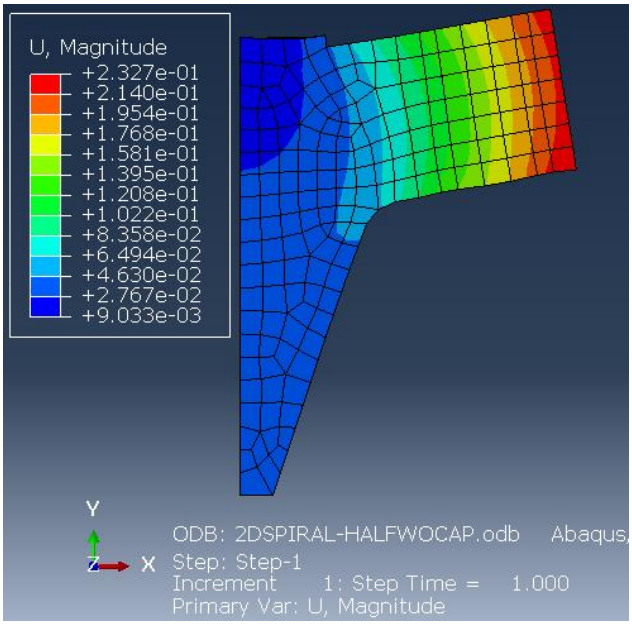

Figure 8.2.3: Displacement results of 2-D Abaqus FEA model of spring wound gasket flange joint

As shown on the plotted contour in Figure 8.2.4, the maximum magnitude of von Mises stress occurred at the fillet of the flange joint with a maximum magnitude of 261.3MPa. Utilizing the CPS4 element resulted in smooth stress and displacement field contours across the 2-D Abaqus FEA model. With the maximum displacement at the outer edge of the flange where the bolt loads occur, the proposed ring gasket experienced a compressive load at the outer edges of the spiral wound gasket for a tight seal in the pipeline.

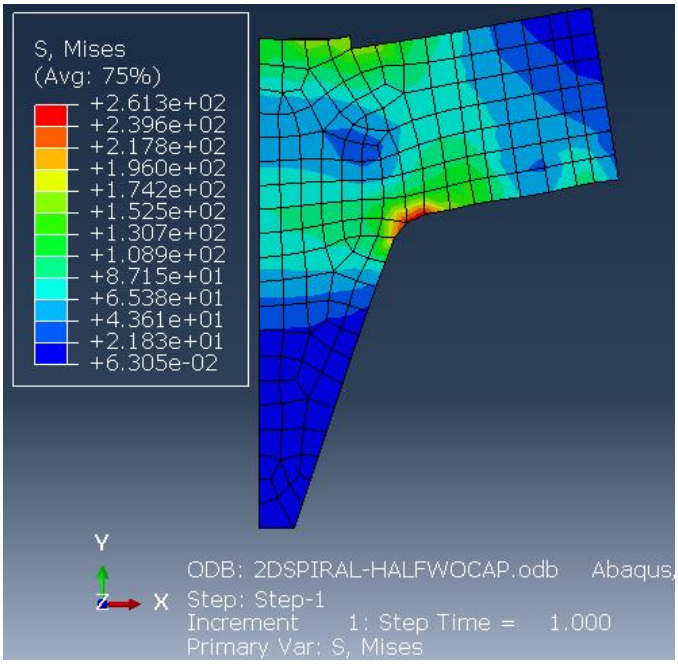

Figure 8.2.4: Stress results of 2-D Abaqus FEA model of proposed flange joint

8.3 2-D MATLAB solver

For the team to program a finite element solver, several simplifications had to be done to the original goal of modeling a gasket between a flange. Ultimately, it was decided to model a two-dimensional cross section of a flange, gasket and bolt, and only model the pressure of the bolt. In addition to being able to more directly leverage techniques taught in the course, the created solver provided an interesting comparison to the more thorough and complex model of Abaqus.

From a software architecture point of view, a finite element solver program was tailored for this specific simplified flange problem in MATLAB. Although much of the code written was specific to this problem, there was a goal to make the code applicable to as many FEM problems as possible. An object-oriented approach was chosen in an attempt to keep as much of the program as general. Often a more primitive MATLAB construct would be wrapped, such as the GlobalStiffnessMatrix type wrapping a sparse matrix. These helper types would also include functions to handle common operations, such as an Add Local Stiffness Matrix function on the Global Stiffness Matrix. Different element types were developed, however only the base Element type and the Triangular 3 Node 2D-Element classes were used for this investigation.

For simplicity, isoparametric 3-node triangles were chosen for the problem. Analytical expressions were derived for the general elements stiffness matrix and load vector (however due to simplifications and constraints on the problem the distributed load vector was not used for the final results). The derivation began by defining the shape functions:

$$N_1 = \xi$$

$$N_2 = \eta$$

$$N_3 = 1 - \xi - \eta$$

Which led to the conversion functions:

$$x(\xi,\eta) = x_1\xi + x_2\eta + x_3(1-\xi-\eta)$$

$$y(\xi,\eta) = y_1\xi + y_2\eta + y_3(1-\xi-\eta)$$

To transform the isoparametric material properties matrix, we need to evaluate a B matrix which equals [9] (note that the source includes a ½ that is factored in later in the computation):

$$\frac{1}{det(J)}\begin{bmatrix} y_2-y_3 & 0 & y_3-y_1 & 0 & y_1-y_2 & 0 \\ 0 & x_3-x_2 & 0 & x_1-x_3 & 0 & x_2-x_1 \\ x_3-x_2 & y_2-y_3 & x_1-x_3 & y_2-y_1 & x_2-x_1 & y_1-y_2 \end{bmatrix}$$

Again, the matrix does not depend on the local variables. To finish the local stiffness matrix, the matrix involving the material properties was found in the literature [10] to be:

$$\Lambda = \frac{E}{1-v^2}\begin{bmatrix} 1 & v & 0 \\ v & 1 & 0 \\ 0 & 0 & \frac{1-v}{2} \end{bmatrix}$$

As none of the matrices and vectors depend on the local variables, they can all be pulled out of the integral of the equation for the element stiffness matrix. The integral in the equation evaluates to one half. This is the matrix that was evaluated for every element:

$$[k]^e = \frac{1}{2}[B]^T[\Lambda][B]det(J)$$

For a distributed load Q, we need to evaluate the integral of the vector of shape functions.

$$\int_0^1 \int_0^{1-\eta} \{N\}\, d\xi\, d\eta = \begin{matrix} \frac{1}{6} \\ \frac{1}{6} \\ \frac{1}{6} \end{matrix}$$

Leading to the evaluation of the local force vector of:

$$\{r\}\hat{}e = Q\, det(J) \begin{matrix} \frac{1}{6} \\ \frac{1}{6} \\ \frac{1}{6} \end{matrix}$$

Finally, concentrated forces would just be applied to the appropriate elements of the global load vector.

The two-dimensional cross section of the flange, gasket and bolt were originally exported from Abaqus, and from that program, a mesh was created in GMSH. There were several issues with this process. First, the size of the element out of GMSH was 1/100th of what it was in Abaqus. This was corrected in the MATLAB code where, when the mesh was read in, all of the node coordinates were multiplied by 100. Also, the export process did not account any curves and fillets on the model.

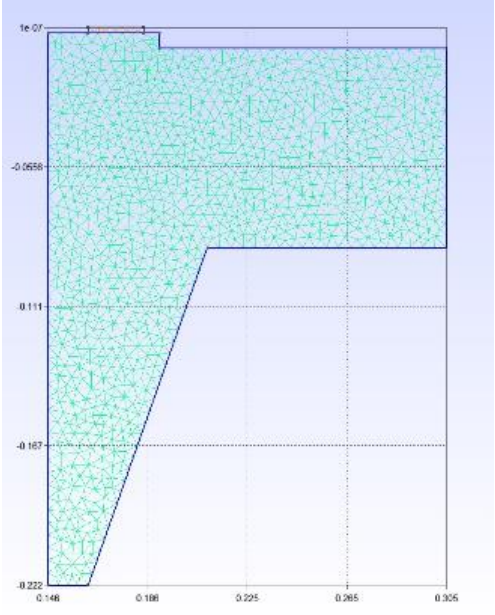

Figure 8.3.1: Mesh for Finite Element Program used in MATLAB

One final issue was that GMSH did not enforce compatibility between the gasket and the flange; there were two completely different sets of nodes for the bottom edge of the gasket and the top of the flange. As such, with the tools at our disposal it was not possible to perform analysis on the gasket with the MATLAB FEM solver. Only the flange under the load of the bolt was modeled.

For simplicity, 3 node triangular elements were used for the mesh, with a maximum unitless value of 0.005. Combined with the material properties used in Abaqus, the local stiffness matrices were derived. Due to the small size that the bolt pressures were applied to, the pressures were converted to a concentrated force at the node closest to the center of the area the bolt.

With the magnitudes of the forces evaluated, they were applied to the node closest to the center of each area the pressure was being applied. The global stiffness matrix wrapped an instance of a sparse matrix that is built into MATLAB, and the global load vector was assembled. For this problem, the pressure was modeled as a boundary condition on the left side of the flange preventing the flange from moving in the X direction. To account for symmetry, the top of the gasket was fixed in the y-direction. The boundary conditions were hard-coded into the program, eliminating rows and columns for node elements that were fixed or where the axis of symmetry cut the cross section. The displacements of the remaining nodes were found by inverting the remainder of the global stiffness matrix and multiplying it with the load vector that remained after eliminating rows due to boundary conditions. The reaction stresses and strains where then computed, and plots of the stress and displacements were generated.

8.4 Comparison between MATLAB code and Abaqus results

Under the bolt load of 199.544MPa, the displacement had a maximum of 0.2203mm. The results for the maximum loading were reasonably close to the Abaqus results, being only 5.3% less than the maximum displacement evaluated in Abaqus.

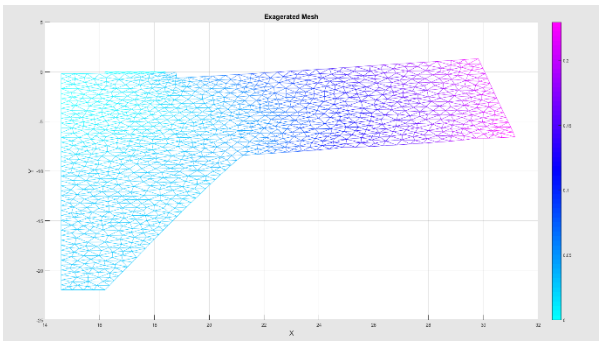

Figure 8.4.1: Mesh under bolt load, displacements exaggerated by a factor of 100

The stress forces on the flange had a similar distribution as the Abaqus model, mainly showing large stress at the lower convex corner and at the boundary condition where the gasket would be. However, the peak value was significantly lower, 45MPa, than what Abaqus evaluated, being nearly an order of magnitude off from Abaqus's value of 261.2MPa. It is strongly suspected that there is an error in the written FEM program causing this discrepancy.

Allowable:

The grade of the flange was of high strength steel Gr.65 with a yield strength of 450MPa. The fastener material yield strength was 725MPa with a tensile strength of 860MPa.

Spiral Wound Gasket (by vendor)

- Minimum Gasket seating stress = 50 MPa
- Optimal gasket seating stress = 122 MPa
- Maximum Gasket seating stress = 300 MPa

Ring type joint for soft iron (by vendor)

- Minimum Gasket seating stress = 235 MPa
- Optimal gasket seating stress = 350 MPa
- Maximum Gasket seating stress = 525 MPa

9.0 Discussion

9.1 Discussion and analysis of results

As anticipated in the 3-D model, there were very high localized stress at the base of the flanges were the loads were applied. This would not have occurred if the cap would also have been modeled to transfer the loads evenly. Therefore, these high stress concentration points were neglected from the analysis when the external loads were applied.

3-D RF spiral wound gasket joint model

The stress on the flange joint prior to application of the was 323MPa at the neck of the flange. Here due to the limitation on the number of nodes the fillet radius of 13mm was not modeled as it would require finer mesh in the region. However, these stresses are well with the allowable of the flange. Also, this was checked on the 2-D model were the fillet radius was modeled and the stress were 261.3MPa.

The maximum stress occurred at the bolts in the model of 426.5MPa well within the yield stress of the bolt of 725MPa. The spiral wound gasket relaxed from 387.5MPa to 138MPa. This satisfied the vendors catalogue minimum gasket seating stress requirement, but as the initial seating stress exceeded the allowable(300MPa) the gasket. The gasket failed to relax from the high initial stress which might have caused the leak. It was found that the bolt load applied initial for the joint make up was very high to make the joint seal during construction. Also, the ASME Post Construction Code (Appendix O) limitation of the allowable relaxation of the spiral wound gasket needed to be checked in further studies. Due to time limitation, this check was not carried out.

Based on the analysis carried out, the raised face gasket failed due to the high load imposed to make this joint seal during its initial stages. This result reinforced the API 14E recommendations that raised face flanges should be used for flanges less than 600# rating.

The stress needed to be lowered by 23%. However, to achieve this, the bolt tension in the initial make-up of the joint should be lowered. Decreasing the bolt load by 23% will bring the joint very close to the lower limit of minimum bolt tension with the upper limit of the gasket's maximum stress satisfied. It was foreseen that these tight margins would cause issues for the site team to implement this solution and may not achieve a leak-free joint with the present external loading. This might be the reason the applied loads were high initially, as they could not get a leak free joint due to the narrow margins. The torqueing tools used to make up the joints itself have a 15-30% error in the applied loads.

2-D Spiral wound gasket joint model

The 2-D Abaqus model was made to check the local stress on the flange joint at the make up condition were within the allowable and to check the solver equation and results.

The flange stress was checked and was found to be within the allowable stress. The inhouse computer program solver also provided the results and was compared with the Abaqus 2-D model proving that the equations were marginally incorrect with further study needed to incorporate the contact elements and gasket closure behavior.

3-D RTJ flange joint

The RTJ model applied the same load as that the Raised face flange with spiral wound gasket was subjected to. The initial bolting load for gasket seating for the RTJ joint showed highest stress were on the bolts as anticipated of 510.4MPa. the flanges saw a maximum stress of 249MPa well within the allowable. Therefore, a 2-D model was not necessary to confirm the maximum stress on the flange. After the external load were applied the maximum stress on the flange other than that of the boundary edges were within the allowable. The bolt stress was also checked and were found to be within the allowable range.

The RTJ joint passed the minimum and maximum seating stress requirements easily. The initial gasket seating stress during bolting up was 480MPa. When the pressure loads were applied the gasket relaxed to 332MPa and finally when the external loads were applied the gasket relaxed to 322.3MPa.

Therefore, the RTJ joint was recommended in this study to be pursued as the way forward as a long-lasting solution.

9.2 Implications for design

The ASME code requirement for the bolt tension applied for the ring type joint might have been used to seal the spiral wound gasket joint. This may have degraded the flange joint performances. Further investigation would need to be carried out by the site team to determine this with the contractor which carried out the bolting works. Therefore, this study proposes the replacement of the existing flange joint and spiral wound gasket with a new with RTJ flange joint with a soft iron gasket.

10.0 References

[1] MSS-SP-44: Pipe Flanges and Flanged Fittings (2017 Edition)

[2] ASME B16.20: Metallic Gaskets for Pipe Flanges (2017 Edition)

[3] A study on the sealing performance of flange joints with gaskets under external bending using finite-element analysis by G Mathan and N Siva Prasad

[4] A study on the sealing performance of bolted flange joints with gaskets using finite element analysis by M. Murali Krishna, M.S. Shunmugam, N. Siva Prasad

[5] Analysis and Testing of a Ring-Joint Flange by Clifford A. Hay, P.E., Warren Brown, Ph.D., P.Eng.

[6] Flexitallic Gasket Design Criteria

[7] Stress Analyses and a Sealing Performance Evaluation of Pipe Flange Connections with Spiral Wound Gaskets under Internal Pressure by Sawa, T., Ogata, N., Nishida, T.

[8] Smith Gasket Brochure

[9] Concepts and Application of Finite Element Analysis (4th Edition), Robert Cook, David Malkus, Michael Plesha, Robert Witt, University of Wisconsin – Madison, 2002

[10] 2D Triangular Elements - http://www.unm.edu/~bgreen/ME360/2D%20Triangular%20Elements.pdf Accessed on 2018 Dec 06

[11] ASME PCC-1 Post Construction Code Guidelines for Pressure Boundary Bolted Flange Joint Assembly

[12] ASME Section VIII Div.1 Boiler and Pressure Vessel Code

[13] Recommended Practice for Design and Installation of Offshore Production Platform Piping Systems. API Recommended Practice 14E (RP 14E) (Fifth Edition)